Article

Harnessing Secondary Coordination Sphere Interactions Enables the Selective Amidation of Benzylic C-H Bonds

Hoimin Jung, Malte Schrader, Dongwook Kim, Mu-Hyun Baik, Yoonsu Park, and Sukbok Chang

J. Am. Chem. Soc., **Just Accepted Manuscript** • DOI: 10.1021/jacs.9b07795 • Publication Date (Web): 26 Aug 2019

Harnessing Secondary Coordination Sphere Interactions Enables the Selective Amidation of Benzylic C–H Bonds

Hoimin Jung,[†,‡] Malte Schrader,[§] Dongwook Kim,[‡,†] Mu-Hyun Baik,[‡,†,*] Yoonsu Park,[‡,†,*] and Sukbok Chang[‡,†,*]

[†]Department of Chemistry, Korea Advanced Institute of Science and Technology (KAIST), Daejeon 34141, South Korea

[‡]Center for Catalytic Hydrocarbon Functionalizations, Institute for Basic Science (IBS), Daejeon 34141, South Korea

[§]Organisch-Chemisches Institut, Westfälische Wilhelms-Universität Münster, Corrensstraße 40, Münster 48149, Germany

ABSTRACT: Engineering site-selectivity is highly desirable especially in C–H functionalization reactions. We report a new catalyst platform that is highly selective for the amidation of benzylic C–H bonds controlled by π-π interactions in the secondary coordination sphere. Mechanistic understanding of the previously developed iridium catalysts that showed poor regioselectivity gave rise to the recognition that the π-cloud of an aromatic fragment on the substrate can act as a formal directing group through an attractive non-covalent interaction with the bidentate ligand of the catalyst. Based on this mechanism-driven strategy, we developed a cationic (η^5-C_5H_5)Ru(II) catalyst with a neutral polypyridyl ligand to obtain a record-setting benzylic selectivity in an intramolecular C–H lactamization in the presence of tertiary C–H bonds at the same distance. Experimental and computational techniques were integrated to identify the origin of this unprecedented benzylic selectivity, and robust linear free energy relationship between solvent polarity index and the measured site-selectivity was found to clearly corroborate that the solvophobic effect drives the selectivity. Generality of the reaction scope and applicability towards versatile γ-lactam synthesis were demonstrated.

Introduction

The selective functionalization of C–H bonds is a central theme in transition metal-based catalysis. In principle, site-selectivity towards a specific C–H bond is dictated by a complex interplay of multiple kinetic and thermodynamic factors.[1] For instance, secondary C–H bonds are sterically less demanding than tertiary counterparts and can therefore be accessed more easily by metal catalysts, generally leading to faster reactions.[2] In some cases, the electronic richness on the tertiary position can effectively stabilize intermediates that derive from C–H bond cleavage to favor activation of the tertiary C–H bond.[3] Unusual electronic structures, such as multiple accessible spin states found in high-valent metal-carbenoids[4] and -nitrenoid[5] species, further complicate the activation mechanisms. As a result, predicting and rationally designing selective C–H bond cleavage reactions has been notoriously difficult.

Catalytic C–H amination is one of the most direct approaches to installing nitrogen functionalities onto organic compounds via C–H functionalization.[6] Recent efforts to harness the power of C–H amination for preparing pharmaceutically active products[7] dramatically increased the complexity of substrates that can be processed giving high levels of control even when other reactive functionalities are present. Selective benzylic C–H amination attracted special attention in this context (Scheme 1a), because the benzylamine scaffold is of particular pharmaceutical importance.[8] Du Bois firstly addressed this issue by designing a sulfamate ester substrate[9] containing benzylic and tertiary C–H bonds positioned at the same distance. In this system, benzylic-to-tertiary (B:T) ratio was shown to be moderate at ~1.5:1,[10] while sterically bulky catalysts enabled selective amidation at the tertiary position.[9,11]

Scheme 1. Site-selective C–H amination via nitrene transfer.

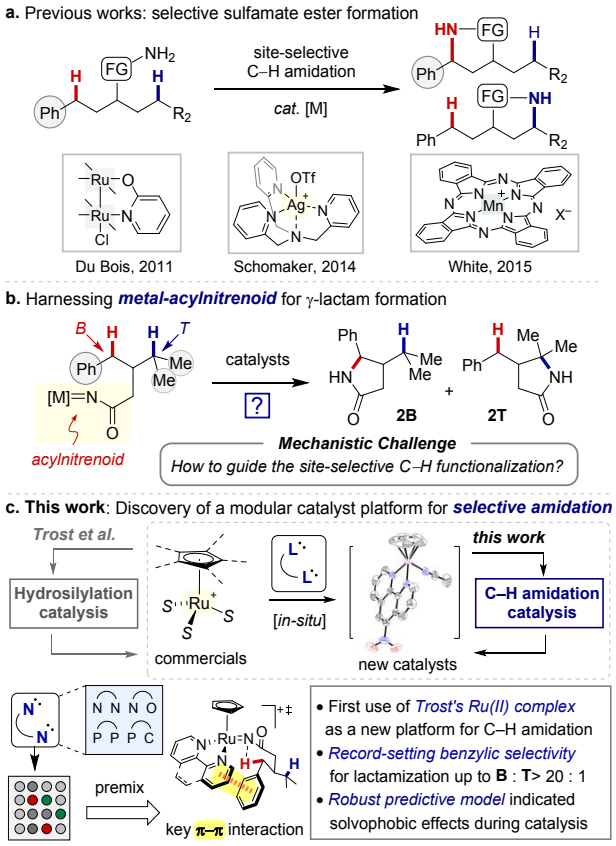

Schomaker reported a remarkable series of silver-based catalysts that facilitate C–H functionalization at the benzylic over tertiary position at a ratio of 5.8:1.[12,13] In addition, White recently showed that iron and manganese-based catalysts can display exceptional selectivity towards

the benzylic position in the introduction of sulfamate ester moieties.[14] While these systems are state-of-art examples of selective catalysis, most of them are confined to sulfamate ester formation. Moreover, strategic concepts for enforcing the benzylic selectivity is scarce at the present.

We recently found that 5-membered cyclic amides can be formed by driving C–H insertion upon accessing the reactive metal-acylnitrenoid intermediates.[15] Experimental and computational analyses validated the closed-shell reactivity of the employed iridium-based catalysts, where singlet metal-nitrenoid species are engaged in electrophilic, two-electron C–H insertion processes. Considering aforementioned issue on the B:T selectivity, we wondered whether selective benzylic C–H amidation could be achieved in the presence of electron-rich tertiary C–H bonds (Scheme 1b). The importance of benzyl-functionalized lactams further motivated us to target such selective catalysis.[16] This pursuit is challenging, however, because there is no rational strategy for distinguishing the benzylic positions in a putative 6-membered cyclic transition state.

Thus, we attempted to construct a conceptual foundation based on the reaction mechanism that may allow for engineering such B:T selectivity. In an iterative search that incorporated insights from both computational and experimental studies, we identified a novel ruthenium catalyst system that displays an exceptional selectivity towards benzylic C–H amidation (Scheme 1c). Specifically, DFT calculations suggested that non-covalent interactions between the catalyst and the substrate may be exploited to direct the reactivity towards the benzylic position. The cationic (η^5-C_5R_5)Ru(II) complexes (R= H or Me), which is a renowned catalyst for Trost's hydrosilylation[17] and allylic substitution[18] reactions, were found to be ideal for this new strategy. This new platform allows for rapidly prepararing a variety of so-far inaccessible catalysts by simply premixing the commercially available metal precursor and neutral ligands on demands. Such operational simplicity was further leveraged for parallel screening of ligand effects, and a novel catalyst was identified that led to unprecedented site-selectivity towards benzylic position with B:T ratios as high as 25:1. Integrated experimental and computational mechanistic studies on the origin of the site-selectivity confirmed the active role of π-π interactions under the Curtin-Hammett situation. The highly reactive yet selective nature of the new system further enabled catalytic production of various γ-lactams from versatile amide agents, 1,4,2-dioxazol-5-ones.

Results and Discussion

Evaluation of B:T selectivity against known catalysts. Initially, we sought to utilize a model substrate that allows for systematically evaluating the performance of various catalysts towards the B:T selectivity. For this purpose, 1,4,2-dioxazol-5-one **1** containing both benzylic and tertiary C–H bonds at the γ- and γ'-positions was selected owing to its robust nature as an acylnitrene precursor.[19] Various catalysts that previously displayed notable reactivity for γ-lactam formation were tested and the results are summarized in Scheme 2. Iridium(III) catalysts bearing either *N,N'* or *N,O*-bidentate ligands (**Ir1** to **Ir4**) offered excellent amidation reactivity, but produced almost equimolecular amount of γ-lactams **2B** and **2T**. Chiral iridium catalysts (**Ir5**[20] and **Ir6**[21]) that previously enabled asymmetric induction afforded diminished reactivity and selectivity. Inspired by the elegant recent work of Yu,[22] the (*p*-cymene)Ru(II)-based catalyst (**Ru1**) was also tested, but it only gave moderate selectivity (**2B**:**2T** = 2.1:1). Displacement of the chiral diamine ligand to aminoquinoline functionalities (**Ru2**) yielded poor regioselectivity, suggesting that none of the currently known catalysts for the γ-lactam formation gives satisfactory results and highlighting the fundamental difficulty in differentiating the benzylic from tertiary C–H bonds mentioned above. Because identifying catalysts capable of effectively carrying out γ-lactam forming reactions is challenging on its own right, a conventional screening of a large diversified set of catalysts is neither possible nor desirable. Thus, we sought to more comprehensively understand the reaction mechanism and identify a conceptual feature that may allow for engineering high levels of B/T selectivity using the acylnitrene intermediate.

Scheme 2. Evaluation of B:T selectivity with previously reported catalysts.[a]

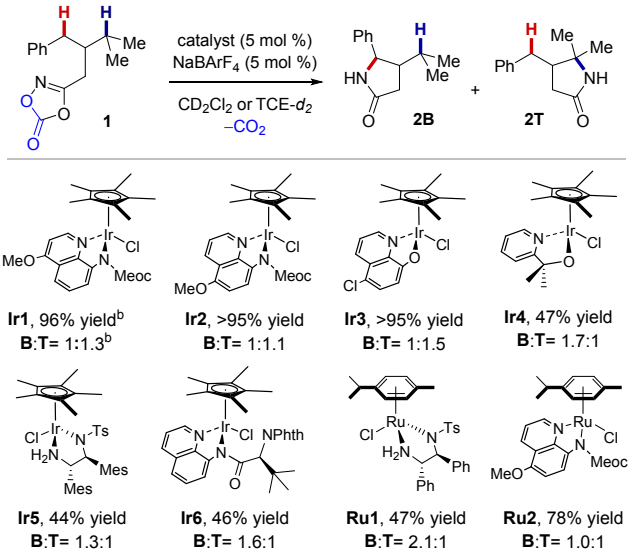

[a]Reactions were performed for 12 hours at room temperature; yields and B:T-selectivities were determined by crude ^{1}H NMR analysis using 1,1,2-trichloroethane as an internal standard. Otherwise stated, single diastereomer was observed for compound **2B**. [b]Retrieved from reference 15. TCE, 1,1,2,2-tetrachloroethane. Meoc, methyloxycarbonyl.

Computer-Aided Design Strategy. Mechanistically, the regioselectivity is determined at the step of C–H insertion, as highlighted in Scheme 3. Previous studies established a mechanism involving the oxidative decarboxylation of the catalyst-substrate adduct **I** to give a highly reactive iridium-acylnitrenoid intermediate **II**.[23] Whereas complex **II** may have several distinct conformers,

II-B and **II-T** illustrated in Scheme 3 are most relevant to the key C–H insertion step leading to the benzylic and tertiary amidation, respectively. Since traversing the 6-membered C–H insertion transition states might irreversibly lead to the corresponding lactam products,[15] the process determining the selectivity can be analyzed by employing the Curtin-Hammett principle that gives control over the two possible reaction pathways.

Scheme 3. Distinctive reaction pathways to **2B** and **2T**.

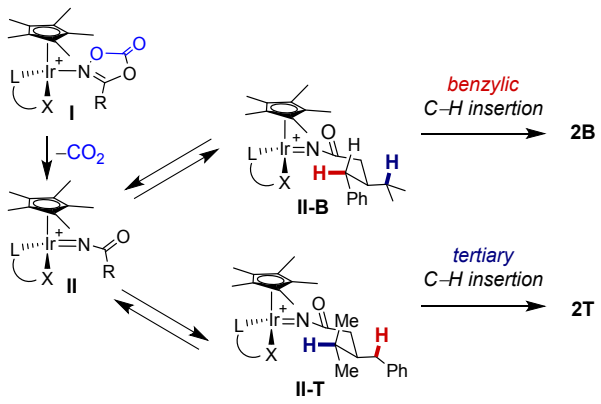

The reaction mechanism was investigated in detail using the representative iridium catalyst **Ir2** at the B3LYP-D3/cc-pVTZ(-f) level of density functional theory[24,25] and the key findings are summarized in Figure 1. As shown in a full reaction energy diagram in Figure S6, the putative iridium-nitrenoid species **II** can be generated from an adduct **I** by traversing the decarboxylation transition state with an activation barrier of 13.2 kcal/mol. Extensive conformational search of the resulting intermediate located two active intermediate conformers **II-B** and **II-T**, which are thermodynamically more stable than their parent linear conformer **II** by 2.8 and 2.3 kcal/mol, respectively, thus identifying **II-B** as the lowest energy intermediate. Complex **II-B** can undergo benzylic C–H insertion with a barrier of 5.2 kcal/mol (**II-B** to **II-B-TS**), whereas tertiary functionalization requires slightly less energy of 4.6 kcal/mol (**II-B** to **II-T**, then to **II-T-TS**). The computed free energy difference between **II-B-TS** and **II-T-TS** ($\Delta\Delta G^{\ddagger}$= 0.6 kcal/mol) taken at face value suggests that the tertiary C–H bond activation is slightly preferred over the benzylic C–H activation, and this finding is consistent with an experimental trend observed in Scheme 2. But, given that these reaction steps have very low barriers of ~5 kcal/mol and follow immediately the likely rate-determining decarboxylation step, these seemingly reasonable agreement between theory and experiment must be evaluated with some caution. Nonetheless, the calculations are fully consistent with the experimental findings and a closer inspection of the factors that determine the C–H bond insertion is justified.

Interestingly, the optimized transition state geometries reveal a critical insight that is useful for a possible catalyst design strategy. As highlighted in Figure 1, there is a potential π-π interactions in the intermediate conformer **II-B** that precedes the benzylic insertion, which is absent in the conformer **II-T**. In **II-B** the phenyl moiety of the substrate is arranged in parallel orientation to the quinoline ligand of the catalyst at a π-π distance of 3.65 Å, well within the expected distance of a π-π stack.[26] This attractive interaction, however, weakens as the bulky phenyl moiety approaches the metal center for the benzylic activation and at the transition state **II-B-TS** the π-π stack is lost, as a detailed analysis of the intrinsic reaction coordinate (IRC) trajectory unambiguously confirmed (Figure S7).

Intrigued by this computational analysis, we envisioned that if the attractive π-π interaction can be maintained throughout the C–H insertion event, it may offer a new way of enhancing the B:T selectivity towards benzylic functionalization in the absence of any coordinating group. As depicted in Scheme 4, we anticipated that the barrier associated with the benzylic activation could be lowered, while the barrier for the tertiary C–H bond remains unaffected. To test this idea, we imagined that an aromatic ligand with an extended π-system may be a reasonable candidate. At the same time, we were also mindful of the electronic structure of the metal-nitrenoid

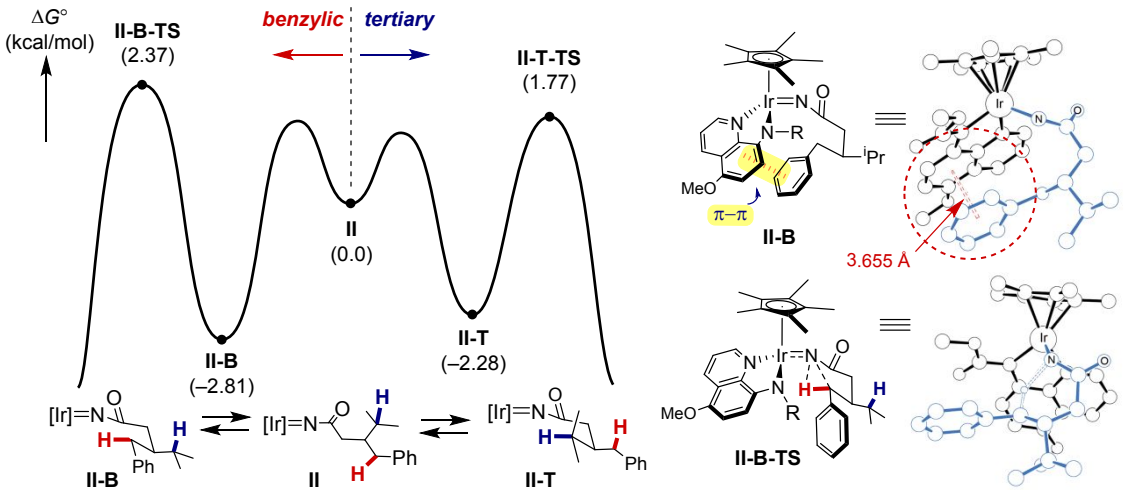

Figure 1. Potential energy profile of the **Ir2** system for B:T selectivity-demanding stages.

species and the influence from the ancillary ligand Cp* because they were previously identified as critical factors in other C–H functionalization reactions.[27] To incorporate these concerns, we sought to systematically examine d^6-based catalysts, such as Ir(III), Rh(III), and Ru(II) complexes that are known to mediate metal-acylnitrenoid formation from carbonylnitrene precursors, e.g. dioxazolones and acyl azides.[28]

Scheme 4. Catalyst design strategy for benzylic selectivity.

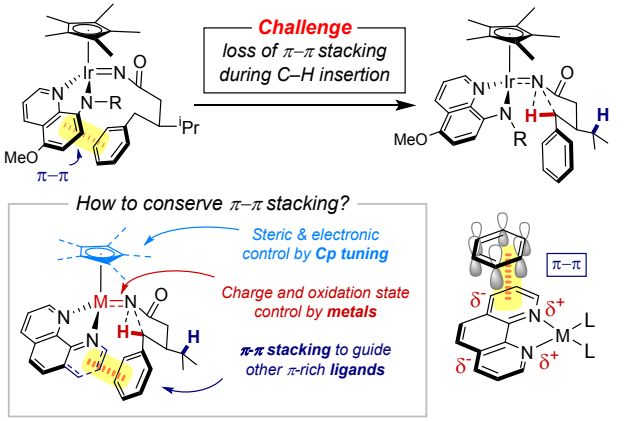

Searching for a new catalyst platform that satisfies the aforementioned criteria, we became interested in polypyridine ligands that have neutral molecular charge and rich aromatic π-clouds in a rigid planar backbone, such as 1,10-phenanthroline (phen). Indeed, free polypyridine compounds are known for participating in π-π interactions with various organic fragments, and the extent of such interaction further increases substantially upon bidentate σ-coordination to a Lewis acidic metal center due to coordinatively induced π-polarization (Scheme 4).[29] Most prominently, Barton demonstrated that the phen functionality in the $[Ru(phen)_3]^{2+}$ complex can readily intercalate into DNA through strong π-π interactions with nucleobase pairs.[30] Interestingly, recent examples in transition metal catalysis accentuated the importance of π-π stacking in catalytic activity and selectivity.[31] Zhu discovered an iron/phen-based catalyst that enables benzylic selective hydrosilylation of styrene derivatives.[32] Mechanistic studies have identified that π-π interaction between a substrate and the catalyst guided the excellent regio-selectivity. In a similar vein, Schomaker and co-workers have found that π-π stacking is operative in silver/polypyridyl amine catalysis for selective C–H amidation of sulfamidate esters.[12b] Computational study suggested that the pyridyl moiety coordinated to a silver catalyst displays active non-covalent interaction through space. In this system, benzylic C–H functionalization is favored over tertiary activation up to 5.8:1 in B:T selectivity.

Reaction development. Motivated by these examples and our own computational analysis, we sought to prepare metal complexes bearing neutral phen ligands to harness potential π-π interactions for lowering the activation barrier for the benzylic C–H cleavage (Scheme 5). Targeted [Cp*Ir(phen)Cl]Cl (**Ir7**) and analogous rhodium (**Rh1**) and ruthenium (**Ru3**) congeners were independently synthesized by reacting metal-chloride dimers and free phen ligand.[33] Catalytic amounts of these complexes were subsequently subjected to a solution of dioxazolone **1** with concomitant addition of sodium organoborate to generate cationic species having one vacant coordination site. To our surprise, the dicationic complexes did not display any reactivity (entries 2-4). Analysis of the crude mixtures indicated that quantitative amount of the starting materials remained unreacted after 12 h at room temperature. We reasoned that this lack of reactivity might be due in part to thermodynamic inaccessibility of dicationic metal-nitrenoid species. Kinetic barrier for the key oxidative decarboxylation is expected to be much higher in energy because of the highly electrophilic nature of putative dicationic metal-nitrenoid intermediate.

Scheme 5. Reaction Development.[a]

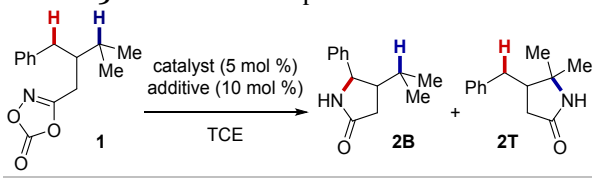

entry	catalyst	addtivie	yield (%)	2B:2T
1	**Ir2**	$NaBAr^F_4$	96	1:1.1
2	**Ir7**	$NaBAr^F_4$	<5	<5
3	**Rh1**	$NaBAr^F_4$	<5	<5
4	**Ru3**	$NaBAr^F_4$	<5	<5
5	**Ru4**	-	61	**7.4**:1
6	**Ru5**	-	80	**8.3**:1
7	$[Cp^*Ru(MeCN)_3](PF_6)$	-	44	1.3:1
8	$[CpRu(MeCN)_3](PF_6)$	-	70	2.0:1
9	**Ru5**[b]	-	88	**14**:1

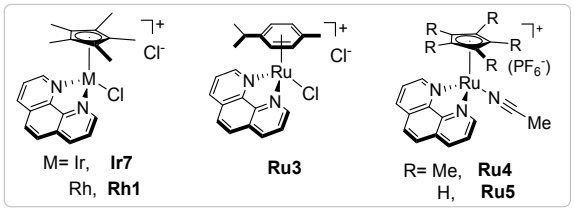

[a]Reactions were performed for 12 h at room temperature; yields and B:T-selectivities were determined by crude ^{1}H NMR analysis using 1,1,2-trichloroethane as an internal standard. [b]Run in hexafluoro-2-propanol (HFIP) solvent.

The inactivity of the dicationic complexes on the lactam formation highlights the importance of catalyst charge on the amidation reactivity. It led us to pursue a new catalyst platform having a d^6 configuration where a molecular charge of +1 could be maintained upon complexation with neutral phen ligand. One possible class of the catalysts that meet this criteria includes a group 8 Cp*Ru(II) complex, which has been mainly utilized as effective pre-catalyst for alkyne hydrosilylation[17] and allylic substitution[18] reactions. In fact, while arene-coordinated ruthenium(II) complexes, such as (*p*-cymene)Ru(II) chloride dimers, have been extensively studied in the C–H amidation chemistry recently,[34] a related Cp*Ru(II) complex has received much

less attention, and there is no literature example for utilizing this type of catalysts for C–H amidation reactions.

The targeted Cp*Ru(II)/phen complex **Ru4** was simply prepared by mixing commercially available solvento-complex $[Cp^*Ru(MeCN)_3](PF_6)$ and phen ligand. To our delight, mono-cationic **Ru4** catalyst indeed displayed amidation reactivity, and afforded the desired γ-lactam products in overall yield of 61% (entry 5, Scheme 5). More significantly, the B:T selectivity was found to be in favor of the benzylic position by as much as 7.4 times. This B:T ratio is remarkable when compared to the reactions with the previously known catalysts shown in Scheme 2. An obvious optimization of this encouraging result is to test the simpler Cp variants. Interestingly, substitution of the Cp* ancillary ligand with Cp groups further enhanced the reactivity and selectivity to afford 80% combined yield and 8.3:1 of the B:T ratio (entry 6). Control reactions in the absence of phen ligand afforded significantly lowered activities (entries 7-8), suggesting that the 1,10-phenanthroline ligand plays an important role in the selectivity determining process, as designed. Utilizing HFIP as solvent gave rise to an even higher selectivity of 14:1 and product yield of 88% (entry 9). Of note, evaluation of solvent effects with the previous catalysts in Scheme 2 gave only a marginal impact on the selectivity, showcasing the unique selectivity of the newly scrutinized CpRu(II) platform.

Scheme 6. Ligand effects on $(\eta^5\text{-}C_5H_5)$Ru(II)-catalyzed C–H amidation of dioxazolones.[a]

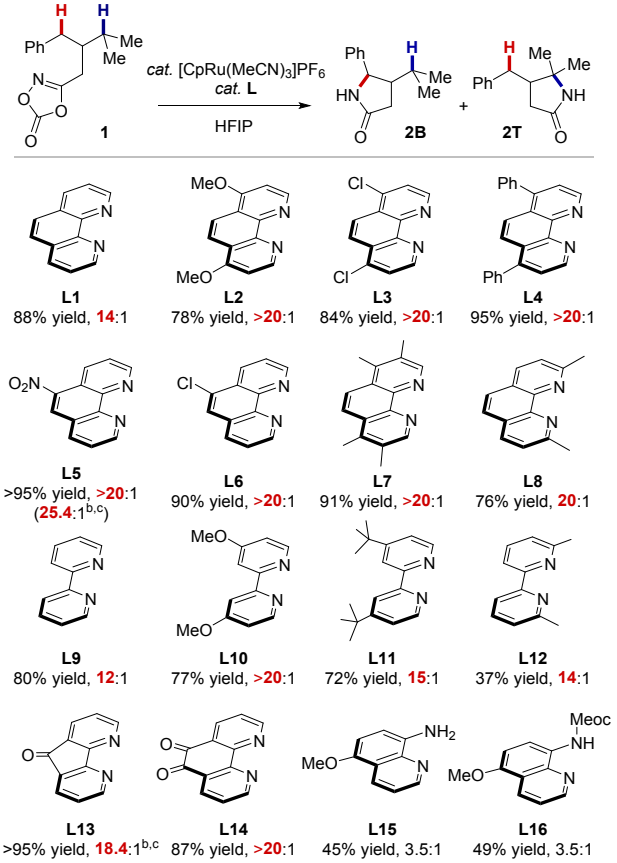

[a]Reactions were performed for 12 h at room temperature; yields and B:T-selectivities were determined by crude ^{1}H NMR analysis using 1,1,2-trichloroethane as an internal standard. [b]Determined by HPLC analysis. [c]Run at 40 °C

We firstly examined commercially available 1,10-phenanthroline derivatives as potential ligands, and the results are summarized in Scheme 6. Electronic variation resulted in high selectivity with variable product yields, possibly due to the electronic perturbation on the π-cloud (**L2** to **L8**). Among them, 5-nitro-1,10-phenanthroline (**L5**) gave quantitative conversion to the benzyl-amidated γ-lactam **2B** with excellent site-selectivity, reaching up to 25.4:1 ratio (**2B**:**2T**), which is arguably a record-setting selectivity in the intramolecular C–H amidation reactions when benzylic and tertiary C–H bonds compete with each other. The ligand pool was further extended to include a related family of bidentate nitrogen donors. Whereas the bipyridyl framework provided variable selectivities and reactivities (**L9** to **L12**), 4,5-diazafluoren-9-one (**L13**) and 1,10-phenanthroline-5,6-dione (**L14**) ligands that had been studied for aerobic oxidation reactions[35] displayed excellent activities towards selective C–H amidation reactions. In comparison, the 8-aminoquinoline scaffold (**L15**, **L16**), which was effective in iridium(III) catalysis,[15] resulted in decreased efficiency and selectivity.

Benzylic selectivity over other reactive positions. We next wondered whether our new catalyst system is tolerant to stereo-electronic perturbations of the substrates. Utilizing the pre-mixing strategy to generate an active catalyst, a score of substrates was subjected to the optimal conditions with ligand **L5** (Figure 2). Installing electron-withdrawing groups on the aromatic moiety eroded the B:T selectivity to some extent. For example, whereas the *p*-chloro substituent displayed excellent regioselectivity (17:1, **3B**), the trifluoromethyl group only gave moderate selectivity (4.9:1, **4B**). Interestingly, notable increase in the selectivity was observed when electron-rich ligand **L2** was used in lieu of **L5**. The use of ligands with electron-donating groups may enhance the proposed π–π interactions with electron-deficient aryl groups in substrates, thus eventually increasing the benzylic selectivity. On the other hand, electron-donating substituents such as methoxy group offered almost exclusive benzylic selectivity (>20:1, **5B** and **6B**). This electronic trend is easy to understand considering the substituent effects on the benzylic bond strengths. Similar qualitative observation was made in a recent study by Schomaker and co-workers in silver-catalyzed selective C–H amidation reactions.[12b] Steric variation on the tertiary moiety afforded excellent benzylic regio-selectivity, as exemplified by a substitution of isopropyl with cyclohexyl group (**7B**). Moreover, a new type of substrate **8** that contains phenylethyl and isobutyl groups at the α-carbon to the dioxazolone moiety also displayed a high level of benzylic selectivity yet with moderate diastereoselectivity (**9B**). Of particular note, otherwise identical reactions with the iridium catalyst (**Ir2**) resulted in poor site-selectivity in most of the cases examined, clearly highlighting extraordinary selectivity by the current ruthenium catalyst system.

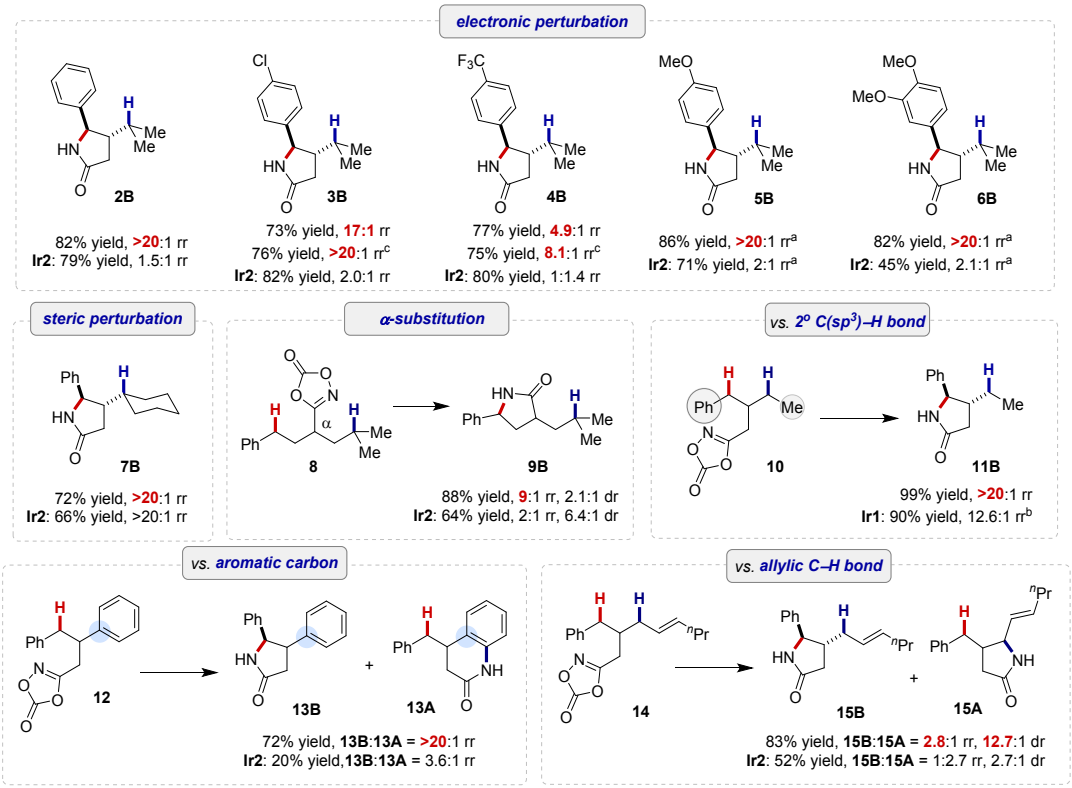

Figure 2. Benzylic selectivity over other reactive sites. Reactions were performed in HFIP solvent for 12 hours at 40 °C; benzylic selectivities were determined by crude ^{1}H NMR analysis; isolated yields. Otherwise noted, single diastereomer was formed upon the reactions. rr, regiomeric ratio; dr. diastereomeric ratio. [a]TCE as solvent. [b]Retrieved from reference 15. [c]**L2** instead of **L5**.

Further elaboration was made with substrates that contain potentially reactive positions. For example, subjecting substrate **10** with γ-secondary bonds gave rise to excellent level of benzylic selectivity. A dioxazolone substrate bearing β-phenyl moiety (**12**) is interesting because benzo-fused δ-lactam **13A** could be formed via an *ipso* spiro-lactamization/skeletal rearrangement sequence.[36] Whereas reaction with **Ir2** indeed gave a mixture of **13B** and **13A**, the current ruthenium system exclusively afforded γ-lactam **13B** in 72% yield. When γ-allylic C–H bonds competes with benzylic functionalization, diastereoselective formation of **15B** was observed albeit only displaying moderate regioselectivity.

Evidences for π-π interactions during catalysis. To further elucidate the mechanistic origin of the unprecedentedly high selectivity towards the benzylic C–H bond, integrated experimental and computational mechanistic studies were conducted. Two independent factors were envisaged to be relevant to inducing the benzylic selectivity: (a) radical character of a putative ruthenium-nitrenoid intermediate, and (b) non-covalent interaction between catalyst and substrate in the selectivity-determining step. At the outset, we sought to characterize the active catalyst. Treatment of tris(acetonitrile) Ru complex with ligand **L5** in TCE solvent immediately generated complex **Ru6** upon concomitant release of two acetonitrile molecules, as monitored by ^{1}H NMR spectroscopy (Scheme 7a). Single crystal of **Ru6** could be obtained after slow diffusion of diethyl ether into saturated acetonitrile solution, and its X ray-crystallographic analysis unambiguously assigned its solid-state structure. Selectivity in the lactam formation with this isolated ruthenium catalyst was observed to be identical (Scheme 7b) when compared to what was found using the catalyst obtained *in situ* by the pre-mixing protocol described in Scheme 6. This result confirms the active involvement of **Ru6** in the catalytic process.

The predominant cleavage of C–H bonds with lower BDE is often taken as an indirect evidence for open-shell reactivity. For example, Che observed a quantitative correlation between reaction rate constants and bond dissociation energies (BDEs) in related stoichiometric C–H amidation reactions via H-atom abstraction.[37] Thus, we were mindful of the possibility that the observed high B:T ratio might arise from the radical character of the putative Ru-nitrenoid intermediate because BDE of benzylic C–H bond (86 kcal/mol) is lower in energy than that of tertiary position (96 kcal/mol).[1] To examine this hypothesis, we performed a series of diagnostic experiments aimed to probe for radical reactions. A catalytic reaction with a substrate **16-d_2** having *syn*-dideuterio group gave a KIE value of 2.2 (Scheme 7c), which is in a similar range with our previously observed KIE of 1.5 for the closed-shell iridium catalysts.[15] Product analysis showed that the diastereomeric lactam **18** that may be formed by generating a carbon-centered radical followed by epimerization, was not detected. Moreover, the catalytic conversion of the enantio-enriched dioxazolone (***S*)-19** afforded a complete

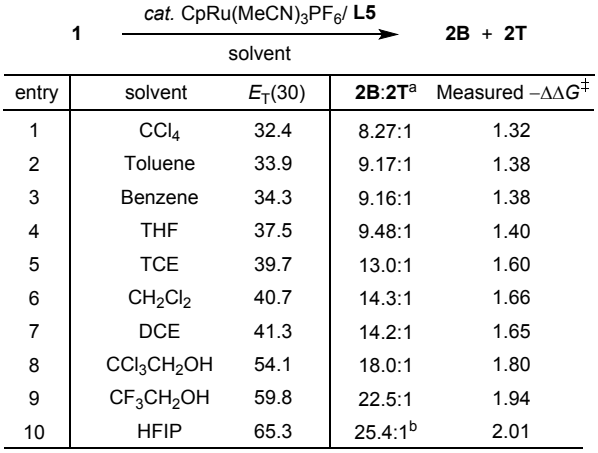

entry	solvent	$E_T(30)$	2B:2T[a]	Measured $-\Delta\Delta G^{\ddagger}$
1	CCl_4	32.4	8.27:1	1.32
2	Toluene	33.9	9.17:1	1.38
3	Benzene	34.3	9.16:1	1.38
4	THF	37.5	9.48:1	1.40
5	TCE	39.7	13.0:1	1.60
6	CH_2Cl_2	40.7	14.3:1	1.66
7	DCE	41.3	14.2:1	1.65
8	CCl_3CH_2OH	54.1	18.0:1	1.80
9	CF_3CH_2OH	59.8	22.5:1	1.94
10	HFIP	65.3	25.4:1[b]	2.01

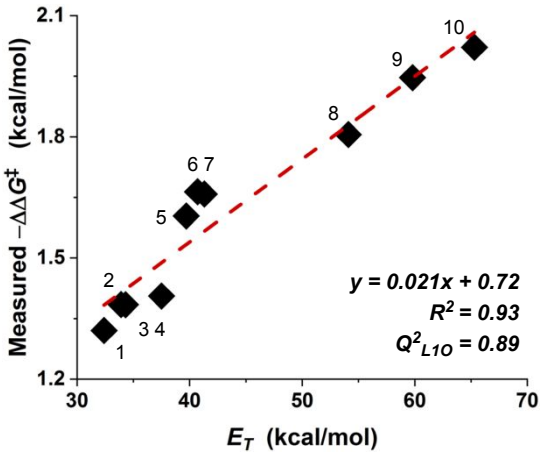

Figure 3. Linear free-energy relationship of the B:T selectivity on a solvent polarity scale. $E_T(30)$ values were retrieved from reference 39b. Measured $-\Delta\Delta G^{\ddagger}$ values were calculated from $-\Delta\Delta G^{\ddagger} = RT\ln([\mathbf{2B}]/[\mathbf{2T}])$ at 313.15 K. [a]Determined by crude ^{1}H NMR analysis. [b]Determined by HPLC analysis. DCE, 1,2-dichloroethane.

retention of stereochemistry, confirmed by chiral HPLC analysis (Scheme 7d). While the thermal generation of a Ru-nitrenoid species having an open-shell state cannot be completely ruled out at the current stage, these experimental results strongly suggest that the Ru-catalyzed reaction follows a closed-shell mechanism.

Scheme 7. Experimental mechanistic studies.

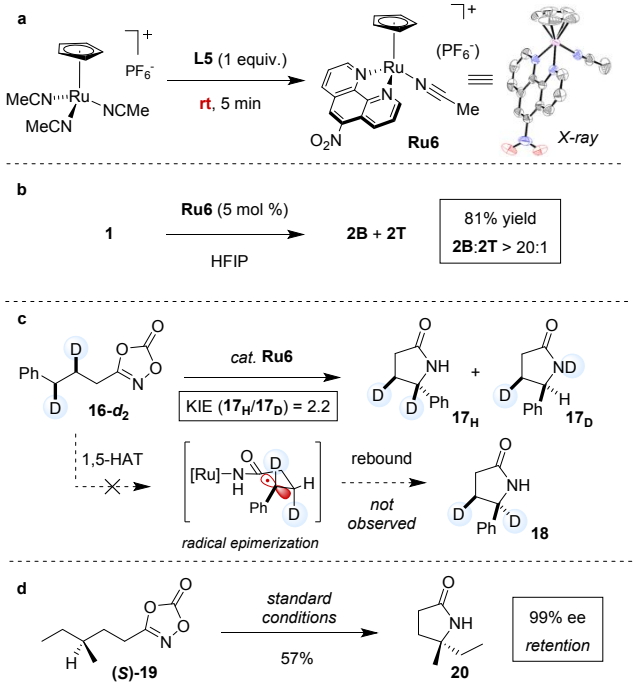

One unanswered question in our proposed mechanism is that under a two-electron mechanism manifold, the tertiary C–H bond cleavage is frequently favored over benzylic functionalization. Representative examples include the Rh(II)-catalyzed C–H amidation by Du Bois[9] and Ir(III)-catalyzed C–H amidation from our laboratory.[15] To rationalize this aspect, we investigated the importance of the interactions in the second coordination sphere. As explained above, the 1,10-phenanthroline ligand contains a delocalized π-cloud that can form a π-π sandwich dimer with aromatic functionalities of the substrate to give stabilization energy in the range of 2~3 kcal/mol.[26c] One way for experimentally probing such interactions is to interrogate the solvent influence on the catalyst activity. In fact, Diederich and co-workers discovered that the magnitude of molecular association between macromolecular cyclophane host and pyrene substantially increases when more polar solvents are employed (Scheme 8a).[38] The observed trend was further quantified by a linear-free energy relationship, where experimentally measured association constants were directly correlated with the empirical solvent polarity parameter, $E_T(30)$.[39] Indeed, Iverson further showed that degree of aromatic π-π interactions between aedamer monomers are positively proportional to the $E_T(30)$ values (Scheme 8b).[40]

Scheme 8. Quantifying solvophobic effects with empirical solvent polarity parameter, $E_T(30)$.

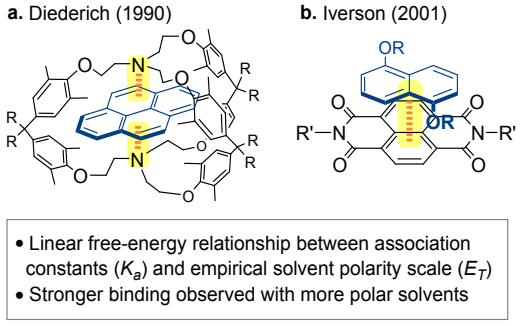

These studies quantitatively showcased solvophobic effects, which states that cohesive force between polar solvent molecules drive strong interactions between non-polar solutes.

Thus, we envisioned that perturbation of the **2B**:**2T** selectivity might be observed if π-π stacking plays an important role in rendering the benzylic selectivity. Typical organic solvents with a wide range of $E_T(30)$ values

were tested and the results are enumerated in Figure 3. While moderate to excellent yields were obtained with the subjected solvents, a clear trend was observed in selectivity that more polar solvents promote reactivity at the benzylic C–H bonds. Specifically, non-polar solvents, such as tetrachloromethane and benzene, displayed selectivities in the range of 9:1, whereas alcoholic solvents afforded much higher selectivities. This observation was quantitatively supported by a linear free energy relationship between solvent polarity indices and experimentally obtained $\Delta\Delta G^{\ddagger}$ value (Figure 3, right). Robust regression model with R^2 and leave-one-out cross-validated R^2 (Q^2_{LiO}) values of 0.93 and 0.89, respectively, implies that polarity of solvent directly impacts on the selectivity. As the $E_T(30)$ values positively correlate with both the extent of π-π stacking[38,40] and the selectivity observed herein, we concluded that the aforementioned hydrophobic effect is critical in the selectivity-determining step for the benzylic C–H amidation.

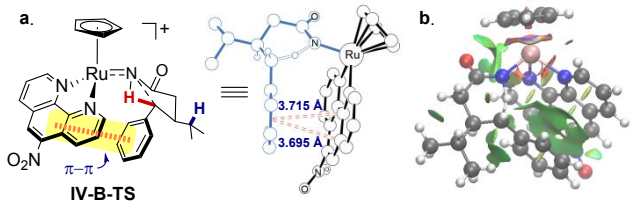

Figure 4. Optimized structure and NCI plot[41] of **IV-B-TS**.

DFT calculations further corroborate the proposed mechanism, as summarized in Figure S8. The calculated intermediate and transition state structures indicate that the π-π stacking interaction is maintained at the intermediate (**IV-B**) and transition states (**IV-B-TS**) to give a barrier that is 1.4 kcal/mol lower than what is required for the C–H activation at the tertiary position (Figure 4a). This free energy difference is in excellent agreement with the experiment. The structures shown in Figure 4a highlights that it is the π-π stacking interaction that arrests the intermediate **IV** into the conformer **IV-B** and allows for overriding the innate preference for the tertiary position. The existence of these non-covalent interactions was further confirmed by the reduced density gradient method devised by Yang and coworkers (Figure 4b).[41]

General applicability to γ-lactam synthesis. Motivated by the exceptional performance of the currently developed Ru catalyst system, we sought to extend the method for the synthesis of γ-lactams in a more general sense. From a synthetic standpoint, our approach to cyclic amide is of general interest because the dioxazolone reactant is easy to prepare from the corresponding carboxylic acid, which is one of the most abundant feedstock chemicals available. As described previously, the challenge associated with the lactamization lies in suppressing Curtius-type rearrangements that affords undesired side-product, while enforcing the desired C–H

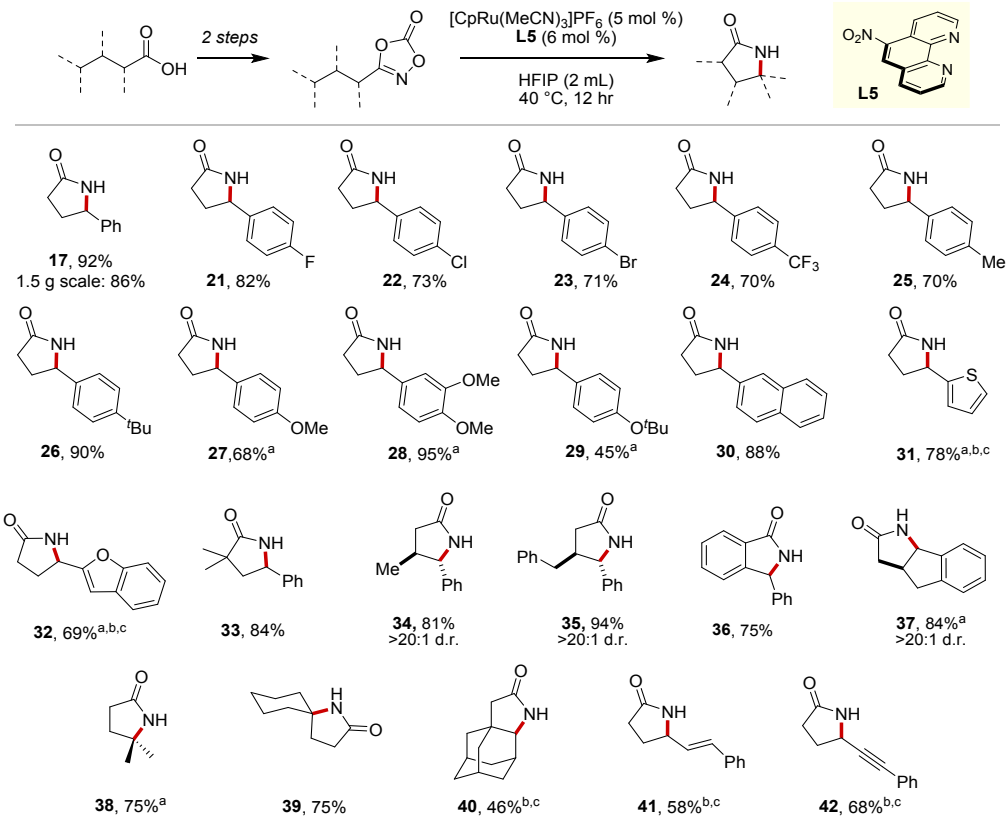

Figure 5. General application to the selective γ-lactam synthesis. [a]1,1,2,2-TCE as a solvent. [b]10 mol % of catalyst was used. [c]Run at 60 °C.

insertion reaction.[15] To test the performance of the new catalyst system, we extensively screened ligands including nitrogen, phosphine, and *N*-heterocyclic carbenes and interrogated their effects on the chemo-selectivity with γ-phenylpropyl dioxazolone as a model substrate, as listed in Scheme S3. As the acetonitrile ligand in the pre-catalyst can be readily displaced with neutral bidentate donors by a priori mixing, we envisioned to perform a rapid screening of ligand effects in the desired amidation. It is interesting that this fast screening effort was not possible in previously employed iridium systems with anionic ligands because base-mediated ligand complexation has always been a bottleneck for the catalyst discovery.[15,20-22,36] Taking full advantage of this pre-mixing technique, we designed a parallel screening protocol that may accelerate the discovery of better catalysts by employing stock solutions of the reaction elements and multi-channel pipettes, which is essentially the procedure utilized in high-throughput experimentation.[42] Specifically, to a series of targeted ligands measured in reaction vials were added a stock solution of $[CpRu(MeCN)_3](PF_6)$ precatalyst via multi-channel pipette and the reactions were placed under vigorous stirring at room temperature for 5 min. Within all tested ligands, *in situ* chelation was confirmed by ^1H NMR monitoring or intense color change. Subsequent addition of a substrate allowed for an interrogation of the ligand influence on the amidation efficiency in a short period of time.

When a premixed Ru/**L5** system was employed, aliphatic dioxazolones containing γ-benzylic C–H bonds were readily converted to cyclic amides in good to excellent yields (Figure 5). Representative γ-phenylpropyl dioxazolone was cyclized to furnish product **17** in 92% yield, and the reaction could be scaled to gram-scale without difficulty. Halide substituents at the *para*-position (**21**-**23**) and electron-withdrawing CF_3 group (**24**) were compatible with the present conditions. Electron-donating substituents such as *p*-alkyl (**25**, **26**) and 3,4-dimethoxy groups (**28**), also offered good to excellent product yields except for *tert*-butoxy group (**29**). In comparison with the previously reported iridium systems,[15] the present ruthenium catalysis shows broader scope on substrates especially bearing electron-donating substituents. Other aromatic groups including napthyl (**30**), thiophenyl (**31**), and benzofuryl (**32**) groups were successfully applicable to the optimal conditions. Notably, sterically encumbered α,α-dimethyl substitutions were tolerated by the ruthenium catalyst (**33**). Of note, we previously observed sluggish conversion when this type of substrates were subjected to iridium-based catalysts owing to undesired decomposition to the corresponding isocyanates.[15] High level of diastereselective cyclization was achieved using dioxazolones having β-substituents (**34**-**37**). Additional types of substrates bearing various γ C–H bonds including tertiary (**38**, **39**), secondary (**40**), allylic (**41**), and propargylic (**42**) groups were also readily cyclized to furnish the corresponding lactams.

Conclusions

We showcased that π-π stacking is an excellent molecular feature to exploit for differentiating the benzylic from tertiary C–H bonds. A mechanistically driven hypothesis enabled the development of a highly modular catalyst system that has been rarely utilized for C–H amidation reactions. By installing a chelating ligand with an extended π-cloud it was possible to maintain a π-π stacking interaction with the phenyl group of the substrate throughout the selectivity determining transition state, which directed the C–H bond functionalization towards the benzylic position. This simple and convenient access to various catalysts is of particular interest because base-mediated ligand complexation with anionic ligands is a prerequisite for most of the previously reported systems. Fully integrated experimental and computational analysis, especially linear free energy relationship between solvent polarity index and the selectivity, indicated that the π-π stacking in secondary coordination sphere plays a pivotal role for inducing the selectivity under the closed-shell reactivity regime. Other factors described in Scheme 4, however, also played additional roles in affording the desired regioselectivity. The change to the neutral ligand required the exchange of the Ir(III)-center of the catalyst with the isolobal Ru(II), and the steric tension at the metal center was also variable between Cp* and Cp supporting ligands. We anticipate that our strategy and discovery could expand the horizon of catalyst development in C–H functionalization reactions and related fields.

ASSOCIATED CONTENT

Supporting Information. The Supporting Information is available free of charge on the ACS Publications website.

Experimental procedures; characterization data; spectra for all new compounds; crystallographic data; Cartesian coordinates of all computed structures (PDF)

AUTHOR INFORMATION

Corresponding Authors

*S.C. Email: sbchang@kaist.ac.kr
*Y.P. Email: yoonsu.park@kaist.ac.kr
*M.-H.B. Email: mbaik2805@kaist.ac.kr

Notes

ORCID:
Hoimin Jung: *0000-0002-3026-6577*
Mu-Hyun Baik: *0000-0002-8832-8187*
Yoonsu Park: *0000-0003-1511-0635*
Sukbok Chang: *0000-0001-9069-0946*

ACKNOWLEDGMENT

We thank support from the Institute for Basic Science (IBS-R10-D1 and IBS-R10-A1) in Korea. We thank Ms. Hyeyun Keum for helpful discussions.

REFERENCES

(1) Xue, X.-S.; Ji, P.; Zhou, B.; Cheng, J.-P., The Essential Role of

Bond Energetics in C–H Activation/Functionalization. *Chem. Rev.* **2017**, *117*, 8622-8648.
(2) (a) Liao, K.; Negretti, S.; Musaev, D. G.; Bacsa, J.; Davies, H. M. L., Site-selective and stereoselective functionalization of unactivated C–H bonds. *Nature* **2016**, *533*, 230-234. (b) Liao, K.; Yang, Y.-F.; Li, Y.; Sanders, J. N.; Houk, K. N.; Musaev, D. G.; Davies, H. M. L., Design of catalysts for site-selective and enantioselective functionalization of non-activated primary C–H bonds. *Nat. Chem.* **2018**, *10*, 1048-1055.
(3) Liao, K.; Pickel, T. C.; Boyarskikh, V.; Bacsa, J.; Musaev, D. G.; Davies, H. M. L., Site-selective and stereoselective functionalization of non-activated tertiary C–H bonds. *Nature* **2017**, *551*, 609-613.
(4) (a) Kornecki, K. P.; Briones, J. F.; Boyarskikh, V.; Fullilove, F.; Autschbach, J.; Schrote, K. E.; Lancaster, K. M.; Davies, H. M. L.; Berry, J. F., Direct Spectroscopic Characterization of a Transitory Dirhodium Donor-Acceptor Carbene Complex. *Science* **2013**, *342*, 351-354. (b) Tindall, D. J.; Werlé, C.; Goddard, R.; Philipps, P.; Farès, C.; Fürstner, A., Structure and Reactivity of Half-Sandwich Rh(+3) and Ir(+3) Carbene Complexes. Catalytic Metathesis of Azobenzene Derivatives. *J. Am. Chem. Soc.* **2018**, *140*, 1884-1893. (c) Hayashi, T.; Tinzl, M.; Mori, T.; Krengel, U.; Proppe, J.; Soetbeer, J.; Klose, D.; Jeschke, G.; Reiher, M.; Hilvert, D., Capture and characterization of a reactive haem–carbenoid complex in an artificial metalloenzyme. *Nat. Catal.* **2018**, *1*, 578-584.
(5) (a) Au, S.-M.; Huang, J.-S.; Yu, W.-Y.; Fung, W.-H.; Che, C.-M., Aziridination of Alkenes and Amidation of Alkanes by Bis(tosylimido)ruthenium(VI) Porphyrins. A Mechanistic Study. *J. Am. Chem. Soc.* **1999**, *121*, 9120-9132. (b) Roizen, J. L.; Harvey, M. E.; Du Bois, J., Metal-Catalyzed Nitrogen-Atom Transfer Methods for the Oxidation of Aliphatic C–H Bonds. *Acc. Chem. Res.* **2012**, *45*, 911-922. (c) Hennessy, E. T.; Betley, T. A., Complex *N*-Heterocycle Synthesis via Iron-Catalyzed, Direct C–H Bond Amination. *Science* **2013**, *340*, 591-595. (d) Glueck, D. S.; Wu, J.; Hollander, F. J.; Bergman, R. G., Monomeric (pentamethylcyclopentadienyl)iridium imido compounds: synthesis, structure, and reactivity. *J. Am. Chem. Soc.* **1991**, *113*, 2041-2054. (e) Varela-Álvarez, A.; Yang, T.; Jennings, H.; Kornecki, K. P.; Macmillan, S. N.; Lancaster, K. M.; Mack, J. B. C.; Du Bois, J.; Berry, J. F.; Musaev, D. G., Rh_2(II,III) Catalysts with Chelating Carboxylate and Carboxamidate Supports: Electronic Structure and Nitrene Transfer Reactivity. *J. Am. Chem. Soc.* **2016**, *138*, 2327-2341. (f) Bart, S. C.; Lobkovsky, E.; Bill, E.; Chirik, P. J., Synthesis and Hydrogenation of Bis(imino)pyridine Iron Imides. *J. Am. Chem. Soc.* **2006**, *128*, 5302-5303. (g) Liu, Y.; Guan, X.; Wong, E. L.-M.; Liu, P.; Huang, J.-S.; Che, C.-M., Nonheme Iron-Mediated Amination of C(sp^3)–H Bonds. Quinquepyridine-Supported Iron-Imide/Nitrene Intermediates by Experimental Studies and DFT Calculations. *J. Am. Chem. Soc.* **2013**, *135*, 7194-7204. (h) Bess, E. N.; DeLuca, R. J.; Tindall, D. J.; Oderinde, M. S.; Roizen, J. L.; Du Bois, J.; Sigman, M. S., Analyzing Site Selectivity in Rh_2(esp)$_2$-Catalyzed Intermolecular C–H Amination Reactions. *J. Am. Chem. Soc.* **2014**, *136*, 5783-5789.
(6) (a) Park, Y.; Kim, Y.; Chang, S., Transition Metal-Catalyzed C–H Amination: Scope, Mechanism, and Applications. *Chem. Rev.* **2017**, *117*, 9247-9301. (b) White, M. C.; Zhao, J., Aliphatic C–H Oxidations for Late-Stage Functionalization. *J. Am. Chem. Soc.* **2018**, *140*, 13988-14009. (c) Zhang, L.; Liardet, L.; Luo, J.; Ren, D.; Grätzel, M.; Hu, X., Photoelectrocatalytic arene C–H amination. *Nat. Catal.* **2019**, *2*, 366-373. (d) Vásquez-Céspedes, S.; Wang, X.; Glorius, F., Plausible Rh(V) Intermediates in Catalytic C–H Activation Reactions. *ACS Catal.* **2018**, *8*, 242-257.
(7) Jeffrey, J. L.; Sarpong, R., Intramolecular C(sp^3)–H amination. *Chem. Sci.* **2013**, *4*, 4092-4106.
(8) (a) Acred, P.; Brown, D. M.; Turner, D. H.; Wilson, M. J., Pharmacology and chemotherapy of ampicillin-a new broad-spectrum penicillin. *Br. J. Pharmacol. Chemother.* **1962**, *18*, 356-369. (b) McGrath, N. A.; Brichacek, M.; Njardarson, J. T., A Graphical Journey of Innovative Organic Architectures That Have Improved Our Lives. *J. Chem. Ed.* **2010**, *87*, 1348-1349.
(9) Fiori, K. W.; Espino, C. G.; Brodsky, B. H.; Du Bois, J., A mechanistic analysis of the Rh-catalyzed intramolecular C–H amination reaction. *Tetrahedron* **2009**, *65*, 3042-3051.
(10) Harvey, M. E.; Musaev, D. G.; Du Bois, J., A Diruthenium Catalyst for Selective, Intramolecular Allylic C–H Amination: Reaction Development and Mechanistic Insight Gained through Experiment and Theory. *J. Am. Chem. Soc.* **2011**, *133*, 17207-17216.
(11) Roizen, J. L.; Zalatan, D. N.; Du Bois, J., Selective Intermolecular Amination of C–H Bonds at Tertiary Carbon Centers. *Angew. Chem., Int. Ed.* **2013**, *52*, 11343-11346.
(12) (a) Alderson, J. M.; Phelps, A. M.; Scamp, R. J.; Dolan, N. S.; Schomaker, J. M., Ligand-Controlled, Tunable Silver-Catalyzed C–H Amination. *J. Am. Chem. Soc.* **2014**, *136*, 16720-16723. (b) Huang, M.; Yang, T.; Paretsky, J. D.; Berry, J. F.; Schomaker, J. M., Inverting Steric Effects: Using "Attractive" Noncovalent Interactions To Direct Silver-Catalyzed Nitrene Transfer. *J. Am. Chem. Soc.* **2017**, *139*, 17376-17386.
(13) (a) Rigoli, J. W.; Weatherly, C. D.; Alderson, J. M.; Vo, B. T.; Schomaker, J. M., Tunable, Chemoselective Amination *via* Silver Catalysis. *J. Am. Chem. Soc.* **2013**, *135*, 17238-17241. (b) Dolan, N. S.; Scamp, R. J.; Yang, T.; Berry, J. F.; Schomaker, J. M., Catalyst-Controlled and Tunable, Chemoselective Silver-Catalyzed Intermolecular Nitrene Transfer: Experimental and Computational Studies. *J. Am. Chem. Soc.* **2016**, *138*, 14658-14667. (c) Corbin, J. R.; Schomaker, J. M., Tunable differentiation of tertiary C–H bonds in intramolecular transition metal-catalyzed nitrene transfer reactions. *Chem. Comm.* **2017**, *53*, 4346-4349. (d) Alderson, J. M.; Corbin, J. R.; Schomaker, J. M., Tunable, Chemo- and Site-Selective Nitrene Transfer Reactions through the Rational Design of Silver(I) Catalysts. *Acc. Chem. Res.* **2017**, *50*, 2147-2158.
(14) (a) Paradine, S. M.; Griffin, J. R.; Zhao, J.; Petronico, A. L.; Miller, S. M.; White, M. C., A manganese catalyst for highly reactive yet chemoselective intramolecular C(sp^3)–H amination. *Nat. Chem.* **2015**, *7*, 987-994. (b) Clark, J. R.; Feng, K.; Sookezian, A.; White, M. C., Manganese-catalysed benzylic C(sp^3)–H amination for late-stage functionalization. *Nat. Chem.* **2018**, *10*, 583-591.
(15) Hong, S. Y.; Park, Y.; Hwang, Y.; Kim, Y. B.; Baik, M.-H.; Chang, S., Selective formation of γ-lactams via C–H amidation enabled by tailored iridium catalysts. *Science* **2018**, *359*, 1016-1021.
(16) (a) Ye, L.-W.; Shu, C.; Gagosz, F., Recent progress towards transition metal-catalyzed synthesis of γ-lactams. *Org. Biomol. Chem.* **2014**, *12*, 1833-1845. (b) Caruano, J.; Muccioli, G. G.; Robiette, R., Biologically active γ-lactams: synthesis and natural sources. *Org. Biomol. Chem.* **2016**, *14*, 10134-10156. (c) Ye, J.; Kalvet, I.; Schoenebeck, F.; Rovis, T., Direct α-alkylation of primary aliphatic amines enabled by CO2 and electrostatics. *Nat. Chem.* **2018**, *10*, 1037-1041. (d) Lei, H.; Conway, J. H.; Cook, C. C.; Rovis, T., Ligand Controlled Ir-Catalyzed Regiodivergent Oxyamination of Unactivated Alkenes. *J. Am. Chem. Soc.* **2019**, *141,* 11864–11869.
(17) (a) Gill, T. P.; Mann, K. R., Photochemical properties of the cyclopentadienyl(η^6-benzene)ruthenium(II) cation. The synthesis and reactions of a synthetically useful intermediate: the cyclopentadienyltris(acetonitrile)ruthenium(II) cation. *Organometallics* **1982**, *1*, 485-488. (b) Trost, B. M.; Pinkerton, A. B., A Mechanistic Dichotomy Leading to a Ruthenium-Catalyzed *cis*-Addition for Stereoselective Formation of (*Z*)-Vinyl Bromides.

Angew. Chem., Int. Ed. **2000**, *39*, 360-362. (c) Trost, B. M.; Ball, Z. T., Markovnikov Alkyne Hydrosilylation Catalyzed by Ruthenium Complexes. *J. Am. Chem. Soc.* **2001**, *123*, 12726-12727. (d) Trost, B. M.; Ball, Z. T., Alkyne Hydrosilylation Catalyzed by a Cationic Ruthenium Complex: Efficient and General Trans Addition. *J. Am. Chem. Soc.* **2005**, *127*, 17644-17655.

(18) (a) Constant, S.; Tortoioli, S.; Müller, J.; Lacour, J., An Enantioselective CpRu-Catalyzed Carroll Rearrangement. *Angew. Chem., Int. Ed.* **2007**, *46*, 2082-2085. (b) Guo, J.-Y.; Minko, Y.; Santiago, C. B.; Sigman, M. S., Developing Comprehensive Computational Parameter Sets To Describe the Performance of Pyridine-Oxazoline and Related Ligands. *ACS Catal.* **2017**, *7*, 4144-4151.

(19) (a) Sauer, J.; Mayer, K. K., Thermolyse und photolyse von 3-subtituierten Δ^2-1.4.2-dioxazolinonen-(5), Δ^2-1.4.2-dioxazolin-thionen-(5) und 4-substituierten Δ^3-1.2.5.3-thiadioxazolin-s-oxiden. *Tetrahedron Lett.* **1968**, *9*, 319-324. (b) Bizet, V.; Buglioni, L.; Bolm, C., Light-Induced Ruthenium-Catalyzed Nitrene Transfer Reactions: A Photochemical Approach towards *N*-Acyl Sulfimides and Sulfoximines. *Angew. Chem., Int. Ed.* **2014**, *53*, 5639-5642. (c) Park, Y.; Park, K. T.; Kim, J. G.; Chang, S., Mechanistic Studies on the Rh(III)-Mediated Amido Transfer Process Leading to Robust C–H Amination with a New Type of Amidating Reagent. *J. Am. Chem. Soc.* **2015**, *137*, 4534-4542. (d) Park, Y.; Jee, S.; Kim, J. G.; Chang, S., Study of Sustainability and Scalability in the Cp*Rh(III)-Catalyzed Direct C−H Amidation with 1,4,2-Dioxazol-5-ones. *Org. Process Res. Dev.* **2015**, *19*, 1024-1029.

(20) Park, Y.; Chang, S., Asymmetric formation of γ-lactams via C–H amidation enabled by chiral hydrogen-bond-donor catalysts. *Nat. Catal.* **2019**, *2*, 219-227.

(21) Wang, H.; Park, Y.; Bai, Z.; Chang, S.; He, G.; Chen, G., Iridium-Catalyzed Enantioselective C(sp^3)–H Amidation Controlled by Attractive Noncovalent Interactions. *J. Am. Chem. Soc.* **2019**, *141*, 7194-7201.

(22) Xing, Q.; Chan, C.-M.; Yeung, Y.-W.; Yu, W.-Y., Ruthenium(II)-Catalyzed Enantioselective γ-Lactams Formation by Intramolecular C–H Amidation of 1,4,2-Dioxazol-5-ones. *J. Am. Chem. Soc.* **2019**, *141*, 3849-3853.

(23) Park, Y.; Heo, J.; Baik, M.-H.; Chang, S., Why is the Ir(III)-Mediated Amido Transfer Much Faster Than the Rh(III)-Mediated Reaction? A Combined Experimental and Computational Study. *J. Am. Chem. Soc.* **2016**, *138*, 14020-14029.

(24) (a) Vosko, S. H.; Wilk, L.; Nusair, M., Accurate spin-dependent electron liquid correlation energies for local spin density calculations: a critical analysis. *Can. J. Phys.* **1980**, *58*, 1200-1211. (b) Becke, A. D., Density-functional exchange-energy approximation with correct asymptotic behavior. *Phys. Rev. A* **1988**, *38*, 3098-3100. (c) Lee, C.; Yang, W.; Parr, R. G., Development of the Colle-Salvetti correlation-energy formula into a functional of the electron density. *Phys. Rev. B* **1988**, *37*, 785-789. (d) Grimme, S.; Antony, J.; Ehrlich, S.; Krieg, H., A consistent and accurate ab initio parametrization of density functional dispersion correction (DFT-D) for the 94 elements H-Pu. *J. Chem. Phys.* **2010**, *132*, 154104. (e) Grimme, S.; Ehrlich, S.; Goerigk, L., Effect of the damping function in dispersion corrected density functional theory. *J. Comput. Chem.* **2011**, *32*, 1456-1465.

(25) (a) Hay, P. J.; Wadt, W. R., *Ab initio* effective core potentials for molecular calculations. Potentials for the transition metal atoms Sc to Hg. *J. Chem. Phys.* **1985**, *82*, 270-283. (b) Wadt, W. R.; Hay, P. J., *Ab initio* effective core potentials for molecular calculations. Potentials for main group elements Na to Bi. *J. Chem. Phys.* **1985**, *82*, 284-298. (c) Dunning, T. H., Gaussian basis sets for use in correlated molecular calculations. I. The atoms boron through neon and hydrogen. *J. Chem. Phys.* **1989**, *90*, 1007-1023.

(26) (a) Hunter, C. A.; Sanders, J. K. M., The nature of π-π interactions. *J. Am. Chem. Soc.* **1990**, *112*, 5525-5534. (b) Sinnokrot, M. O.; Valeev, E. F.; Sherrill, C. D., Estimates of the *Ab Initio* Limit for π−π Interactions: The Benzene Dimer. *J. Am. Chem. Soc.* **2002**, *124*, 10887-10893. (c) Wheeler, S. E.; Houk, K. N., Substituent Effects in the Benzene Dimer are Due to Direct Interactions of the Substituents with the Unsubstituted Benzene. *J. Am. Chem. Soc.* **2008**, *130*, 10854-10855. (d) Orlandi, M.; Coelho, J. A. S.; Hilton, M. J.; Toste, F. D.; Sigman, M. S., Parametrization of Non-covalent Interactions for Transition State Interrogation Applied to Asymmetric Catalysis. *J. Am. Chem. Soc.* **2017**, *139*, 6803-6806.

(27) Piou, T.; Romanov-Michailidis, F.; Ashley, M. A.; Romanova-Michaelides, M.; Rovis, T., Stereodivergent Rhodium(III)-Catalyzed cis-Cyclopropanation Enabled by Multivariate Optimization. *J. Am. Chem. Soc.* **2018**, *140*, 9587-9593.

(28) (a) Hwang, Y.; Park, Y.; Chang, S., Mechanism-Driven Approach To Develop a Mild and Versatile C–H Amidation through Ir^{III} Catalysis. *Chem. - Eur. J.* **2017**, *23*, 11147-11152. (b) Shin, K.; Ryu, J.; Chang, S., Orthogonal Reactivity of Acyl Azides in C–H Activation: Dichotomy between C–C and C–N Amidations Based on Catalyst Systems. *Org. Lett.* **2014**, *16*, 2022-2025. (c) Lei, H.; Rovis, T., Ir-Catalyzed Intermolecular Branch-Selective Allylic C–H Amidation of Unactivated Terminal Olefins. *J. Am. Chem. Soc.* **2019**, *141*, 2268-2273. (d) Knecht, T.; Mondal, S.; Ye, J.-H.; Das, M.; Glorius, F., Intermolecular, Branch-Selective, and Redox-Neutral Cp*IrIII-Catalyzed Allylic C−H Amidation. *Angew. Chem., Int. Ed.* **2019**, *58*, 7117-7121. (e) Burman, J. S.; Harris, R. J.; B. Farr, C. M.; Bacsa, J.; Blakey, S. B., Rh(III) and Ir(III)Cp* Complexes Provide Complementary Regioselectivity Profiles in Intermolecular Allylic C–H Amidation Reactions. *ACS Catal.* **2019**, *9*, 5474-5479.

(29) (a) Miyamura, K.; Mihara, A.; Fujii, T.; Gohshi, Y.; Ishii, Y., Unusually Strong Interactions Mediated by Both π-π Stacking and CH-π Interactions Present in the Dimer of Nickel(II) Complex Coordinated with *n*-Butyl-Substituted Salen. *J. Am. Chem. Soc.* **1995**, *117*, 2377-2378. (b) Mukhopadhyay, U.; Choquesillo-Lazarte, D.; Niclós-Gutiérrez, J.; Bernal, I., A critical look on the nature of the intra-molecular interligand π,π-stacking interaction in mixed-ligand copper(II) complexes of aromatic side-chain amino acidates and α,α′-diimines. *CrystEngComm* **2004**, *6*, 627-632. (c) Sredojević, D. N.; Tomić, Z. D.; Zarić, S. D., Evidence of Chelate−Chelate Stacking Interactions in Crystal Structures of Transition-Metal Complexes. *Crystal Growth & Design* **2010**, *10*, 3901-3908. (d) Martinez, C. R.; Iverson, B. L., Rethinking the term "pi-stacking". *Chem. Sci.* **2012**, *3*, 2191-2201.

(30) Barton, J. K.; Danishefsky, A.; Goldberg, J., Tris(phenanthroline)ruthenium(II): stereoselectivity in binding to DNA. *J. Am. Chem. Soc.* **1984**, *106*, 2172-2176.

(31) Neel, A. J.; Hilton, M. J.; Sigman, M. S.; Toste, F. D., Exploiting non-covalent π interactions for catalyst design. *Nature* **2017**, *543*, 637-646.

(32) Hu, M.-Y.; He, Q.; Fan, S.-J.; Wang, Z.-C.; Liu, L.-Y.; Mu, Y.-J.; Peng, Q.; Zhu, S.-F., Ligands with 1,10-phenanthroline scaffold for highly regioselective iron-catalyzed alkene hydrosilylation. *Nat. Commun.* **2018**, *9*, 221.

(33) (a) Gutsulyak, D. V.; van der Est, A.; Nikonov, G. I., Facile Catalytic Hydrosilylation of Pyridines. *Angew. Chem., Int. Ed.* **2011**, *50*, 1384-1387. (b) Lee, S.-H.; Gutsulyak, D. V.; Nikonov, G. I., Chemo- and Regioselective Catalytic Reduction of *N*-Heterocycles by Silane. *Organometallics* **2013**, *32*, 4457-4464.

(34) (a) Arockiam, P. B.; Bruneau, C.; Dixneuf, P. H., Ruthenium(II)-Catalyzed C–H Bond Activation and Functionalization. *Chem. Rev.* **2012**, *112*, 5879-5918. (b) Shang, M.; Zeng, S.-H.; Sun, S.-Z.; Dai, H.-X.; Yu, J.-Q., Ru(II)-Catalyzed *ortho*-C–H Amination of Arenes and Heteroarenes at Room

Temperature. *Org. Lett.* **2013**, *15*, 5286-5289. (c) Thirunavukkarasu, V. S.; Raghuvanshi, K.; Ackermann, L., Expedient C–H Amidations of Heteroaryl Arenes Catalyzed by Versatile Ruthenium(II) Catalysts. *Org. Lett.* **2013**, *15*, 3286-3289. (d) Bhanuchandra, M.; Yadav, M. R.; Rit, R. K.; Kuram, M. R.; Sahoo, A. K., Ru(II)-catalyzed intermolecular *ortho*-C–H amidation of aromatic ketones with sulfonyl azides. *Chem. Comm.* **2013**, *49*, 5225-5227. (e) Zheng, Q.-Z.; Liang, Y.-F.; Qin, C.; Jiao, N., Ru(II)-catalyzed intermolecular C–H amidation of weakly coordinating ketones. *Chem. Comm.* **2013**, *49*, 5654-5656. (f) Li, J.; Warratz, S.; Zell, D.; De Sarkar, S.; Ishikawa, E. E.; Ackermann, L., *N*-Acyl Amino Acid Ligands for Ruthenium(II)-Catalyzed *meta*-C–H *tert*-Alkylation with Removable Auxiliaries. *J. Am. Chem. Soc.* **2015**, *137*, 13894-13901. (g) Raghuvanshi, K.; Zell, D.; Rauch, K.; Ackermann, L., Ketone-Assisted Ruthenium(II)-Catalyzed C–H Imidation: Access to Primary Aminoketones by Weak Coordination. *ACS Catal.* **2016**, *6*, 3172-3175.

(35) (a) Campbell, A. N.; White, P. B.; Guzei, I. A.; Stahl, S. S., Allylic C−H Acetoxylation with a 4,5-Diazafluorenone-Ligated Palladium Catalyst: A Ligand-Based Strategy To Achieve Aerobic Catalytic Turnover. *J. Am. Chem. Soc.* **2010**, *132*, 15116-15119. (b) Wendlandt, A. E.; Stahl, S. S., Bioinspired Aerobic Oxidation of Secondary Amines and Nitrogen Heterocycles with a Bifunctional Quinone Catalyst. *J. Am. Chem. Soc.* **2014**, *136*, 506-512.

(36) Hwang, Y.; Park, Y.; Kim, Y. B.; Kim, D.; Chang, S., Revisiting Arene C(sp^2)−H Amidation by Intramolecular Transfer of Iridium Nitrenoids: Evidence for a Spirocyclization Pathway. *Angew. Chem., Int. Ed.* **2018**, *57*, 13565-13569.

(37) Leung, S. K.-Y.; Tsui, W.-M.; Huang, J.-S.; Che, C.-M.; Liang, J.-L.; Zhu, N., Imido Transfer from Bis(imido)ruthenium(VI) Porphyrins to Hydrocarbons: Effect of Imido Substituents, C−H Bond Dissociation Energies, and $Ru^{VI/V}$ Reduction Potentials. *J. Am. Chem. Soc.* **2005**, *127*, 16629-16640.

(38) Smithrud, D. B.; Diederich, F., Strength of molecular complexation of apolar solutes in water and in organic solvents is predictable by linear free energy relationships: a general model for solvation effects on apolar binding. *J. Am. Chem. Soc.* **1990**, *112*, 339-343.

(39) (a) Dimroth, K.; Reichardt, C.; Siepmann, T.; Bohlmann, F., Über Pyridinium-*N*-phenol-betaine und ihre Verwendung zur Charakterisierung der Polarität von Lösungsmitteln. *Liebigs Ann. Chem.* **1963**, *661*, 1-37. (b) Cerón-Carrasco, J. P.; Jacquemin, D.; Laurence, C.; Planchat, A.; Reichardt, C.; Sraïdi, K., Solvent polarity scales: determination of new $E_T(30)$ values for 84 organic solvents. *J. Phys. Org. Chem.* **2014**, *27*, 512-518.

(40) Cubberley, M. S.; Iverson, B. L., ^{1}H NMR Investigation of Solvent Effects in Aromatic Stacking Interactions. *J. Am. Chem. Soc.* **2001**, *123*, 7560-7563.

(41) Johnson, E. R.; Keinan, S.; Mori-Sánchez, P.; Contreras-García, J.; Cohen, A. J.; Yang, W., Revealing Noncovalent Interactions. *J. Am. Chem. Soc.* **2010**, *132*, 6498-6506.

(42) Shevlin, M., Practical High-Throughput Experimentation for Chemists. *ACS Med. Chem. Lett.* **2017**, *8*, 601-607.

TOC graphic placeholder